

Near perfect solar absorption in ultra-thin-film GaAs photonic crystals

Cite this: DOI: 10.1039/c3ta13655h

Sergey Eyderman,^{*a} Alexei Deinega^a and Sajeev John^{ab}

We present designs that enable a significant increase of solar absorption in ultra-thin (100–300 nm) layers of gallium arsenide. In the wavelength range from 400–860 nm, 90–99.5% solar absorption is demonstrated depending on the photonic crystal architecture used and the nature of the packaging. It is shown that using only two hundred nanometer equivalent bulk thickness of gallium arsenide, forming a slanted conical-pore photonic crystal (lattice constant 550 nm, pore diameter 600 nm, and pore depth 290 nm) packaged with SiO₂ and deposited on a silver back-reflector, one can obtain a maximum achievable photocurrent density (MAPD) of 26.3 mA cm⁻² from impinging sunlight. This corresponds to 90% absorption of all available sunlight in the wavelength range 400–860 nm. Our optimized photonic crystal design suggests that increasing the equivalent bulk thickness of GaAs beyond 200 nm leads to almost no improvement in solar absorption, while reducing it to 100 nm causes less than 10% reduction in MAPD. Light-trapping in the 200 nm conical pore photonic crystal provides solar absorption exceeding the Lambertian limit over the range of 740–840 nm. The angular dependence of the MAPD for both S- and P-polarizations is also investigated and shows no substantial degradation in the range 0–30°. More dramatic light-trapping and solar absorption is demonstrated in photonic crystals consisting of conical nanowires. Using 200 nm equivalent bulk thickness of GaAs (lattice constant 500 nm, cone base diameter 200 nm, and cone height 4.77 μm) packaged in SiO₂ and deposited on a silver back-reflector, an MAPD of nearly 27 mA cm⁻² is found. This corresponds to absorption of 96% of all available sunlight in the wavelength range 400–860 nm. A clear separation of the solar spectrum along the length of each nanowire is also evident. In the absence of SiO₂ packaging, this MAPD increases to 28.8 mA cm⁻², in excess of the corresponding Lambertian limit of 28.2 mA cm⁻². Most remarkably we find that, if the equivalent bulk thickness of GaAs is increased to 300 nm, nearly 100% of relevant sunlight is absorbed by the conical nanowire photonic crystal.

Received 11th September 2013
Accepted 23rd October 2013

DOI: 10.1039/c3ta13655h

www.rsc.org/MaterialsA

1. Introduction

Solar cells offer a direct way to convert sunlight into electricity. Recently, a considerable amount of research has focused on improving their power conversion efficiency while decreasing the amount of material required for photo-generation of electrical carriers. Gallium arsenide (GaAs) solar cells^{1–3} offer an alternative active material to widely used wafer-based silicon solar cells.⁴ Solar cells made of GaAs have both advantages and disadvantages. Firstly, GaAs has a direct electronic band gap in contrast to crystalline silicon, which has an indirect band gap.⁵ Consequently GaAs absorbs sunlight on shorter distance scales within its allowed band as compared to silicon. While the larger electronic band gap of GaAs leads to less photocurrent generation than silicon, this is more than compensated by the larger open circuit voltage of GaAs solar cells. The current world

record for high efficiency solar cells is held by thin-film GaAs.^{6,7} The main disadvantage of using GaAs is its high cost. Therefore, it is exigent to consider ultra-thin (<200 nm) films of GaAs in low-cost solar cells. However, this reduction in the volume of active material requires efficient light-trapping techniques^{8,9} and improved anti-reflection capabilities^{10–15} in order to match the solar absorption realized in thicker films. Such light-trapping and antireflection can be achieved through nano-structuring of the active material. Light-trapping in thin-film photonic crystals^{16,17} offers opportunities to surpass the performance of conventional thick solar cells. This is possible through a combination of improved solar absorption and more effective carrier collection on length scales smaller than the carrier diffusion length. In this way, thin photonic crystal active layers provide a unique opportunity for both photonic and electronic management in third generation of solar cells.

In this paper, we demonstrate that GaAs photonic crystals consisting of periodic arrays of conical nano-pores or conical nano-wires with equivalent bulk thickness in the range of 100–200 nm can absorb up to 96% of all available sunlight in

^aDepartment of Physics, University of Toronto, 60 St. George Street, Toronto, Ontario, M5S 1A7, Canada. E-mail: sergey.eyderman@utoronto.ca

^bDept. of Physics, King Abdulaziz University, Jeddah, Saudi Arabia

the wavelength range of 400–860 nm, over a broad range of incident angles. With 300 nm of GaAs, sculpted into the form of a conical nanowire photonic crystal, 99.5% of sunlight in this wavelength range can be absorbed. This suggests considerable reduction in the volume of GaAs required in solar cells, while retaining or even exceeding the power conversion efficiencies of thicker and more costly cells.

Despite the advantages of photonic crystal based light trapping, few papers have considered this opportunity in the context of pure GaAs. Recently it was suggested¹ to couple light into a smooth untextured GaAs thin-film using a photonic crystal monolayer of resonant dielectric nano-spheres. These nano-spheres would be deposited on top of a thin cell resting on a silver back reflector. In the case of a 500 nm thick GaAs solar cell, the highest photo-current density obtained (with 500 nm diameter hexagonally close-packed nano-spheres on top) was $J = 26 \text{ mA cm}^{-2}$. This provided only a 3.2% enhancement compared with a flat GaAs solar cell with double antireflection coating, where the current density $J = 25.2 \text{ mA cm}^{-2}$.¹ In contrast, our slanted conical *nano-pore* photonic crystal, packaged in SiO₂, using only 200 nm of GaAs, combines the effects of light trapping and graded index anti-reflection to provide a maximum achievable photo-current density (MAPD) of 26.3 mA cm^{-2} . In the case of the optimized nano-sphere architecture,¹ the same MAPD required using 2.5 times the volume of GaAs compared to our conical *nano-pore* photonic crystal. Moreover, our conical *nanowire* photonic crystal solar cells, using only 200 nm of GaAs, surpass both of these values and provide nearly $J = 28 \text{ mA cm}^{-2}$.

2. Electromagnetic simulation

Numerical simulations were performed using the finite-difference time-domain (FDTD) method¹⁸ with the help of the Electromagnetic Template Library.^{19–22} We use a standard scheme of FDTD calculation in which propagation of a wave impulse through the structure is modeled. During the numerical experiment, the amplitudes of the reflected and transmitted waves are recorded, transformed to the frequency domain and normalized by the incident spectrum. In this way, we directly obtain the transmission $T(\omega)$ and reflection $R(\omega)$ coefficients. The absorption coefficient for given light frequency ω , incident angle and polarization is initially inferred using the conservation of energy:

$$A(\omega) = 1 - T(\omega) - R(\omega) \quad (1)$$

The absorption coefficient is then independently and directly evaluated using the formula

$$A = \frac{\int \omega \epsilon_0 \text{Im}(\epsilon) |E|^2 dx dy dz}{\int \text{Re}[E_0 \times H_0^*] \cdot \mathbf{n} dx dy} \quad (2)$$

Here, ω is the angular frequency, E is the electric field amplitude calculated at each point of a computational grid located within GaAs, ϵ is the frequency-dependent and complex dielectric permittivity of GaAs, E_0 and H_0 are electric and magnetic vectors

of the incident plane wave, \mathbf{n} is a normal unit vector, and the superscript * indicates the complex conjugate. It is verified that both the direct and indirect methods for calculating the absorption give identical results.

The maximum achievable photocurrent density (MAPD), in which all generated carriers are assumed to be collected, is calculated by integrating the simulated absorption with incident solar Air Mass 1.5 Global Spectrum²³ intensity $I(\lambda)$ over the required wavelength range. Assuming that each absorbed photon provides a single electron–hole pair that is separated across a P–N junction and collected without recombination loss, we obtain the maximum achievable short circuit current for the AM 1.5 solar spectrum in the spectral window $[\lambda_{\min}, \lambda_{\max}]$, all collimated into normal incidence:

$$J_{\lambda_{\min}}^{\lambda_{\max}} = \int_{\lambda_{\min}}^{\lambda_{\max}} \frac{e\lambda}{hc} I(\lambda) A(\lambda) d\lambda \quad (3)$$

Here, $I(\lambda)$ is the incident AM 1.5 light intensity, $A(\lambda)$ is the absorption coefficient obtained according to eqn (1) and (2), h is Planck's constant, e is the electronic charge, and c is the speed of light. The experimental data on the GaAs dielectric permittivity is taken from ref. 5 (see Appendix for the details).

The optimization process is as follows. First we calculate absorption coefficients in the wavelength range of 400–860 nm using formula (1) for various radii and lattice constants, keeping the same equivalent bulk thickness. The structure is placed on a perfectly conducting mirror. The absorption coefficient is obtained much more quickly from (1) than from (2). Substituting the calculated absorption into (3) we create an optimization map for the MAPD. However, eqn (1) yields an absorption in the whole structure, including possible parasitic absorption in the substrate. If a realistic silver back-reflector (rather than a perfect conductor) is used, eqn (1) leads to a slight overestimate of the MAPD. Therefore when the optimal radius and lattice constant are found, we recalculate the absorption in GaAs using formula (2), substituting the perfect conductor with a realistic silver mirror. Since the intrinsic absorption of silver is not high, the typical difference in the MAPD between the perfect mirror case and silver is only about $0.7\text{--}0.8 \text{ mA cm}^{-2}$ in the specified wavelength range.

3. Maximal short-circuit current in conical nano-pore arrays

The maximum achievable photo-current density MAPD is an alternative measure of the total amount of AM 1.5 sunlight absorbed in a given structure. For 100% absorption of sunlight in GaAs in the range of 400–860 nm, the MAPD corresponds to 29.1 mA cm^{-2} .

For calibration purposes, we first provide the absorption characteristics of a free-standing bulk GaAs slab (without a mirror) with the thickness varied in the range of 100–2000 nm. Calculating the absorption coefficient using formula (1) and (3) in the spectral range [400–860 nm] we obtain (assuming all sunlight is collimated at normal incidence) the MAPD dependence on the film thickness. The result is shown in Fig. 1. The

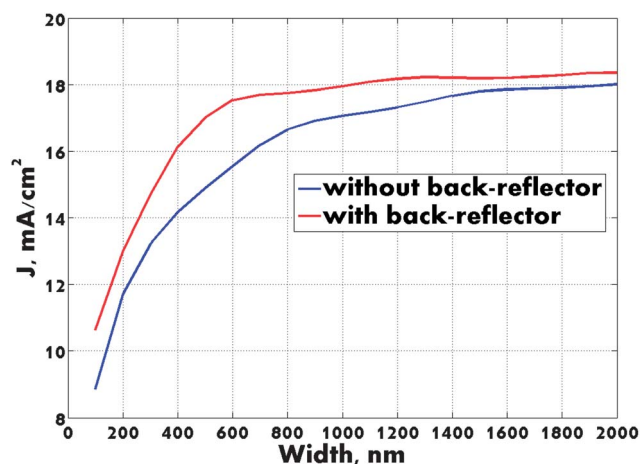


Fig. 1 Maximum achievable photocurrent density (collimated AM 1.5 sunlight at normal incidence) versus the thickness of the GaAs slab with and without a perfect back-reflector in the spectral range [400–860 nm] (red and blue curves, respectively).

maximal short circuit current is only $J = 18.0 \text{ mA cm}^{-2}$, using 2000 nm of GaAs. This corresponds to 62% absorption of incoming sunlight in the wavelength range of 400–860 nm. Adding the perfect mirror on the bottom, we achieve $J = 18.5 \text{ mA cm}^{-2}$ for the same thickness and wavelength range, which is only 64% absorption of incoming sunlight.

These unstructured GaAs architectures suffer from inadequate light trapping and antireflective properties. For an ultra-thin slab (200 nm thick), the majority of the incident light is transmitted or reflected rather than absorbed. Using this volume of GaAs, sculpted into the form of a photonic crystal, we obtain roughly 100% improvement in the generated photocurrent density.

In this section we consider structures consisting of a periodic array of nano-pores in ultra-thin films of GaAs. As shown earlier for silicon solar cells,¹⁶ slanted conical pores provide a more effective graded average refractive index to incoming sunlight and exhibit stronger antireflective properties than their straight counterparts. Since the intrinsic absorptive properties of GaAs are very high, we begin the optimization process for the short circuit current of GaAs solar cells from a thin film perforated with slanted conical nano-pores arranged in a square lattice with the equivalent bulk thickness of 100 nm filled with glass ($n = 1.45$) and placed on a perfectly conducting back-reflector. The result for linearly polarized sunlight at normal incidence is shown in Fig. 2. The maximal short circuit current obtained is $J = 23.2 \text{ mA cm}^{-2}$ in the spectral range [400–860 nm]. Using twice the volume of GaAs as above leads to the MAPD increase from 23.2 to 27.0 mA cm^{-2} .

We also optimized the short circuit current for the slanted conical pore geometry using an equivalent bulk thickness of GaAs of 0.3 μm . In this case, the optimal parameters are $r = 400 \text{ nm}$ and $a = 600 \text{ nm}$ (overall height of cones is 441 nm) yielding $J = 27.7 \text{ mA cm}^{-2}$. This is only a 2.5% improvement relative to the 0.2 μm equivalent bulk thickness case. A further increase of the equivalent bulk thickness of GaAs provides a negligible improvement of the short circuit current. In Fig. 3 we present

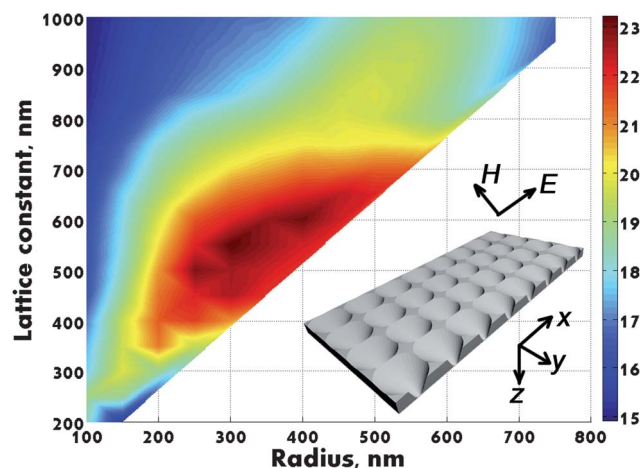


Fig. 2 Short circuit current optimization for a 100 nm GaAs photonic crystal (collimated AM 1.5 sunlight at normal incidence with electric field polarized in the x-direction) in the spectral range [400–860 nm]. The crystal consists of slanted conical holes in bulk gallium arsenide arranged in a square lattice and filled with glass. The photonic crystal slab rests on a perfectly conducting substrate of 100 nm width. For an equivalent bulk thickness of GaAs of 0.1 μm , optimal parameters are $r = 300 \text{ nm}$ and $a = 550 \text{ nm}$. The overall height of the GaAs structure is 140 nm. The color bar on the right indicates MAPD in units of mA cm^{-2} . The maximal short circuit current obtained is $J = 23.2 \text{ mA cm}^{-2}$.

the dependence of the MAPD on the equivalent bulk thickness of GaAs in the spectral range [400–860 nm] for air and glass packaging, respectively. It is seen that for an equivalent bulk thickness less than 350 nm, photonic crystals with glass packaging perform better than their counterparts in which the conical pores are filled with air. However, the graph illustrates a reversal of this tendency beyond 350 nm due to the balance

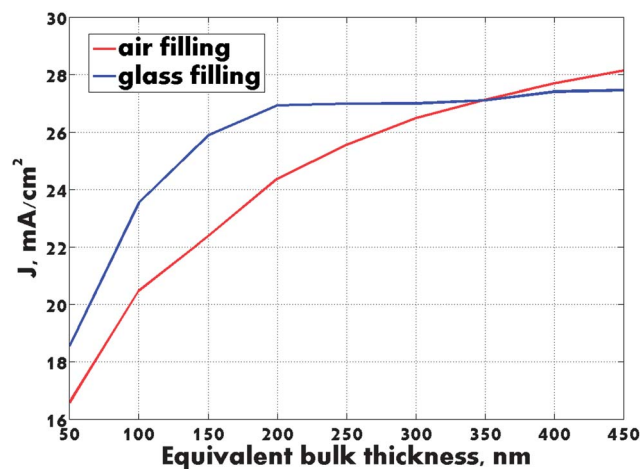


Fig. 3 Maximum achievable photocurrent density versus the equivalent bulk thickness of the conical pore GaAs photonic crystal in the spectral range [400–860 nm] for glass packaging and air filling. The radius of slanted cones is $r = 300 \text{ nm}$ and the lattice constant is $a = 550 \text{ nm}$, which is optimal at equivalent bulk thicknesses of 100 nm and 200 nm. Further optimization is possible at other thicknesses. Each photonic crystal slab rests on a perfectly conducting back-reflector. The red curve corresponds to air-filled slanted cones and the blue curve corresponds to glass-filled pores.

between light-trapping and anti-reflection effects. For small thickness, better light trapping is achieved by filling pores with glass. Adding glass increases the average refractive index of the structure which shifts the photonic band structure downward in frequency, causing more effective light coupling to the parallel-to-interface modes. For larger thickness, antireflection plays an increasingly crucial role. Antireflection is better achieved by the graded refractive index provided air pores, which matches the air boundary at the top of the photonic crystal.

As we discussed in Section 2, the optimal values of MAPD obtained using a perfectly conducting mirror are modified slightly when using a more realistic silver back-reflector. Using the optimal radius and lattice constant found for the perfect conductor, we now calculate the absorption in GaAs using formula (2) with a real silver substrate. The corresponding MAPD is then recalculated using (3). Here we consider the case of the equivalent bulk thickness of GaAs of 0.2 μm . Absorption in GaAs according to (2) (excluding absorption by silver) gives the MAPD of 26.3 mA cm^{-2} which corresponds to 90% absorption of all available sunlight in GaAs in the wavelength range 400–860 nm. This is only slightly below the value of 27.0 mA cm^{-2} obtained using the perfect conductor earlier.

In Fig. 4, we present a comparison of the absorption spectrum in the slanted conical nano-pore photonic crystal with the statistical ray trapping benchmark (also referred to as the Lambertian limit^{16,17}) for a solar cell with the equivalent bulk thickness of 200 nm of GaAs. The absorption coefficient in the statistical ray trapping limit is given by¹⁶

$$A = 1 - \frac{1}{4n^2L\alpha} \quad (4)$$

Here $n = 3.8$ is the real part of the refractive index of gallium arsenide, $\alpha = 4\pi k/\lambda$ is the absorption coefficient (where k is an

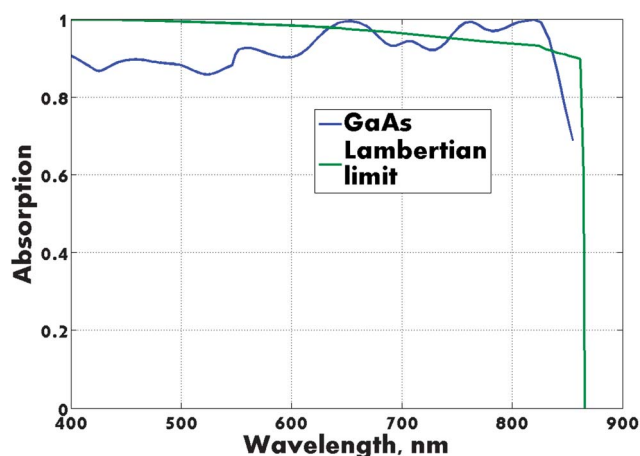


Fig. 4 Comparison of the absorption spectrum obtained for the GaAs slanted conical nano-pore photonic crystal with SiO_2 packaging placed on the perfect conducting back reflector with the Lambertian statistical ray trapping benchmark in the spectral range [400–860 nm] for an equivalent bulk thickness of GaAs of 0.2 μm . The top radius of slanted cones is $r = 300$ nm, the lattice constant is $a = 550$ nm and the cone height is 290 nm. The MAPD for our photonic crystal is = 27.0 mA cm^{-2} , compared to 28.2 mA cm^{-2} in the Lambertian limit and 29.1 mA cm^{-2} if 100% of sunlight is absorbed.

imaginary part of the refractive index of GaAs), and L is the thickness of GaAs. The reference green curve in Fig. 4 for “ $4n^2$ light trapping”^{16,17} is obtained by inserting the experimentally measured values of α for GaAs. Using (4) and substituting it into (3) we obtain $J = 28.2$ mA cm^{-2} for the statistical ray trapping limit in the spectral range [400–860 nm] and an equivalent bulk thickness of GaAs $L = 200$ nm. This very high value is an artifact of neglecting all reflection losses as sunlight initially impinges on the solar cell. This leads to an unrealistically high MAPD in the range of 400–600 nm for the Lambertian benchmark. On the other hand, our realistic modeling of the GaAs conical pore photonic crystal reveals significant reflection in the 400–600 nm range due to the large real part of the dielectric function of GaAs.

The arguments^{16,17} leading to eqn (4) for statistical light trapping were originally intended for conventional slabs where the light absorbing region is typically much thicker than the average wavelength. For photonic crystal films with thicknesses comparable to or smaller than the wavelength, the ray-optics picture and many of the key assumptions in the statistical ray trapping picture are no longer applicable. It was shown earlier that the Lambertian limit can be surpassed in silicon solar cells, even after integrating over the solar spectrum.¹⁶ In Fig. 4 it is shown that the absorption in GaAs calculated for the case of cones filled with SiO_2 exceeds the “Lambertian benchmark” over the partial spectral range [740–840 nm] resulting in a 5% enhancement relative to the MAPD calculated using (4). The difficulty in surpassing the Lambertian limit over the entire spectral range of interest is due to the unrealistic treatment of specular reflection in the $4n^2$ statistical ray trapping limit, which is particularly evident in the wavelength range 400–600 nm.

The microfabrication of conical nano-pore photonic crystals offers an interesting and challenging opportunity in materials chemistry. One approach is to create a single sheet (mold) of the required photonic crystal architecture using reactive ion etching in a material such as silicon. Alternatively, the initial mold can be synthesized using a combination of optical lithography in a photo-resist²⁴ followed by deposition of SiO_2 and silicon into the void regions of the template photonic crystal formed by development of the exposed photo-resist.^{25,26} The silicon-based conical nano-pore photonic crystal sheet can be formed into a large roll that acts as a nano-imprint stamp. This stamp can then imprint the required photonic crystal architecture onto large sheets of a sacrificial polymeric material. GaAs can then be epitaxially deposited into the void regions of the sacrificial polymeric photonic crystal.²⁷ In this way, very large areas of the desired nano-pore GaAs solar cell structure can be manufactured. In the case of nano-wire photonic crystals, well known deposition methods such as vapor-to-liquid-to-solid phase epitaxy can be used to grow conical wires of GaAs.²⁸

4. Angular response of MAPD in nano-pore photonic crystal

A vital aspect of solar cell performance is the ability to absorb sunlight at off-normal incidence for both polarizations, over a wide angular range. In Fig. 5 we present the angular

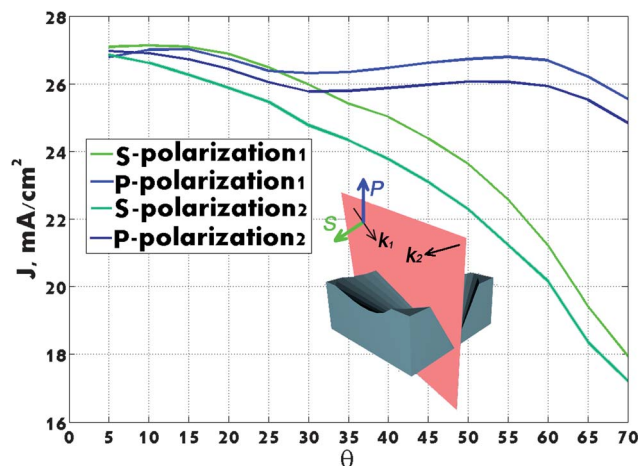


Fig. 5 Angular response of the solar cell for the spectral range [400–860 nm] with the geometry shown in the inset of Fig. 2 with a perfectly conducting back-reflector and SiO_2 packaging. The photonic crystal slab rests on a perfect conducting substrate of 200 nm width. For an equivalent bulk thickness of GaAs of 0.2 μm , optimal parameters are $r = 300$ nm and $a = 550$ nm. Vectors k_1 and k_2 indicate directions of the incident wave in the plane of incidence (see inset). For S-polarized light, the electric field oscillates perpendicular to this plane and for P-polarized light the electric field oscillates within this plane.

distribution of the MAPD for the spectral range [400–860 nm] for the geometry depicted in the inset of Fig. 2 with a perfect conducting back-reflector and SiO_2 packaging. For each incidence angle θ and each polarization channel, it is assumed that the entire AM 1.5 solar spectrum is collimated in that specific angle and channel. Fig. 5 demonstrates that no substantial degradation in the MAPD occurs at least up to $\theta = 30^\circ$ for various polarizations. Both polarization channels yield strong off-normal MAPD characteristics, with p-polarization exceeding s-polarization MAPD for angles of more than 30° from normal incidence.

5. Solar cell architecture

In this section we consider the effect of electrical contacts and GaAs surface passivation on the maximum achievable photocurrent density.²⁹ We incorporate a transparent, conducting indium tin oxide (ITO) ($n = 1.9$) top contact. We coat the surface of the GaAs conical pore array with a thin (10 nm) layer of $\text{Al}_{0.4}\text{Ga}_{0.6}\text{As}$ ⁵ to reduce the surface recombination velocity (SRV).³⁰ As before, we fill the cones with SiO_2 for packaging. The top surface of the SiO_2 as protective packaging is given a sinusoidal modulation chosen to account for a rippling effect of the SiO_2 when deposited on the photonic crystal surface. The final design of this solar cell is presented in Fig. 6.

For passivation of GaAs, the surface of each pore is coated with a layer of AlGaAs of 10 nm width. For this purpose we took $\text{Al}_{0.4}\text{Ga}_{0.6}\text{As}$ with material parameters given in ref. 5.

According to ref. 29 this type of coating gives an SRV of 2900 cm s^{-1} at the interface between the GaAs and $\text{Al}_{0.4}\text{Ga}_{0.6}\text{As}$ interface, which is comparable with an SRV for the silicon–silica interface.³⁰ We have shown, in the case of silicon-based

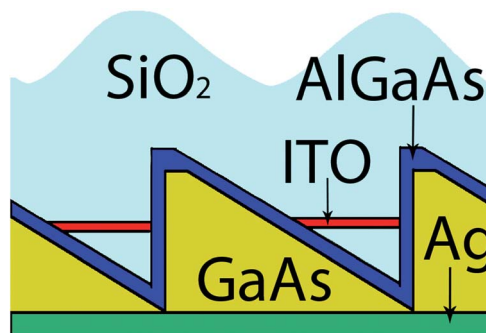


Fig. 6 Perpendicular slice of slanted conical pores in bulk gallium arsenide arranged in a square lattice and filled with glass. The photonic crystal slab rests on a silver substrate of 100 nm width. The height of GaAs protrusions is 0.29 μm (for a 0.2 μm equivalent bulk thickness of GaAs). The radius of cones and the lattice constant are $r = 300$ nm and $a = 550$ nm. The ITO contacts (refractive index $n = 1.9$) represent planar disks of 50 nm width at the middle of each cone. The surface of each pore is coated with a layer of $\text{Al}_{0.4}\text{Ga}_{0.6}\text{As}$ of 10 nm width. The top surface of SiO_2 packaging is given a sinusoidal modulation of 150 nm in minimum and 300 nm in maximum height, respectively, above the top of the GaAs protrusions.

photonic crystal solar cells,^{31,33} that by optimizing the P–N junction geometry and including a passivation layer (with SRV similar to that given above), it is possible to achieve short circuit current densities close to the calculated MAPDs.

This modification of our initial structure leads to a slight decrease in MAPD due to additional reflection from the ITO contact. For the structure shown in Fig. 6 we achieve $J = 24.9$ mA cm^{-2} , which corresponds to 86% of absorption in the spectral range [400–860 nm]. In the case of the flat-top solar cell with conical holes filled with SiO_2 we get $J = 24.85$ mA cm^{-2} , which practically coincides with the case of sinusoidal glass modulation on the top.

6. Conical nanowire photonic crystals

An alternative approach to light-trapping in photonic crystal solar cells consists of nanowire arrays.³² The extremely large surface areas of these systems can be offset by use of a radial P–N junction geometry that rapidly separates photo-generated positive and negative charge carriers and reduces recombination losses.³³ Recently, record high power conversion efficiency has been demonstrated in III–V semiconductor nanowire arrays.³⁴

In the present section, we consider a periodic array of straight, conical nanowires of gallium arsenide, packaged with glass. We show that GaAs nanowire cones are slightly more effective in trapping and absorbing light than their conical-pore counterparts described above. This is distinct from the case of silicon solar cells, where conical pore photonic crystals absorbed more sunlight than an equivalent volume of nanowires.¹⁶

The MAPD map in the case of an equivalent bulk thickness of GaAs of 200 nm is shown in Fig. 7. Here the straight nano-cone array rests on a perfect conductor back-reflector. The maximal short circuit current obtained is $J = 27.8$ mA cm^{-2} for the optimized choice of lattice constant $a = 500$ nm and cone base

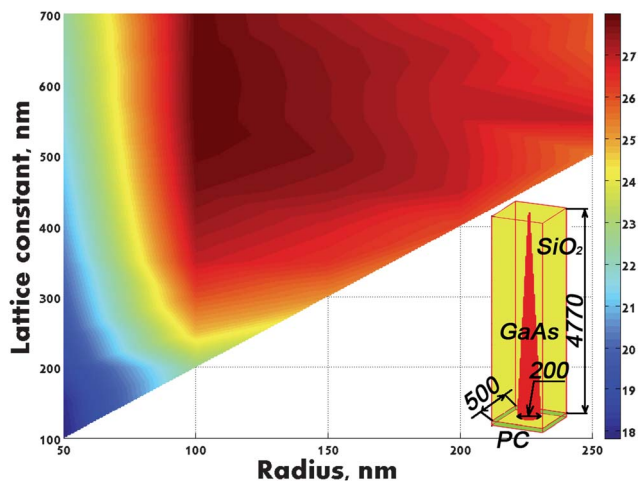


Fig. 7 Short circuit current optimization in the spectral range [400–860 nm] (collimated AM 1.5 sunlight at normal incidence polarized along lattice vector connecting nearest neighbor cone base centers) for straight conical nanowires made of gallium arsenide arranged in a square lattice embedded in glass. The photonic crystal slab rests on a perfect conductor back-reflector of 100 nm width. For an equivalent bulk thickness of GaAs of 0.2 μm , optimal parameters are $r = 100$ nm and $a = 500$ nm. The overall height of the conical nanowires is 4.77 μm . All parameters are given in the inset. The color bar on the right indicates MAPD in units of mA cm^{-2} . The maximal achievable photo-current density obtained is $J = 27.8 \text{ mA cm}^{-2}$. This corresponds to absorbing nearly 96% of available sunlight in the wavelength range considered.

radius $r = 100$ nm. The overall height of the conical nanowires is 4.77 μm . We note that while the above numbers give a mathematical optimum, there is a broad range of choices for the radius and the lattice constant for which the MAPD exceeds 26.0 mA cm^{-2} .

Unlike the case of nano-pores, the introduction of asymmetry (slant) to the nano-wire photonic crystal has a negligible

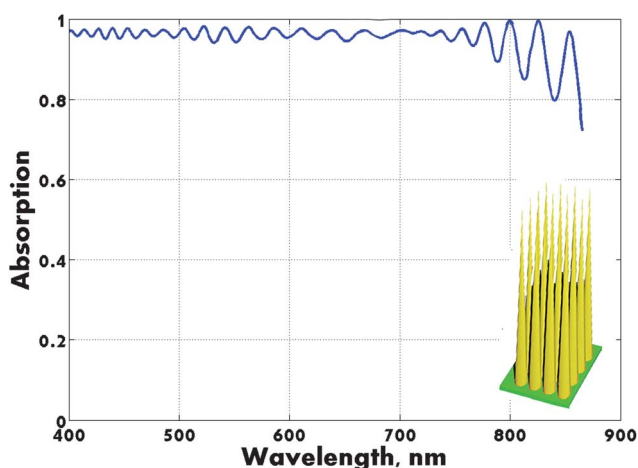


Fig. 8 The absorption spectrum in the range [400–860 nm] obtained for the GaAs photonic crystal made of straight nano-cones, packaged in SiO_2 , placed on the perfect conductor back-reflector for an equivalent bulk thickness of 200 nm of GaAs. The radius of each cone base is $r = 100$ nm and the lattice constant is $a = 500$ nm. The conical nanowire array is depicted in the inset.

effect on the optimum MAPD. The MAPD for corresponding, optimized, *slanted*, conical nanowires is $J = 27.9 \text{ mA cm}^{-2}$. This is practically the same as the symmetric case presented in Fig. 7.

In Fig. 8, we plot the absorption spectrum for the geometry shown in Fig. 7.

Clearly the optimized structure possesses very strong antireflection and absorption properties. Over a broad wavelength range (400–860 nm) it exhibits almost 96% absorption of incoming sunlight. The reflection losses and the weak oscillations in the spectrum are largely due to the flat top SiO_2 packaging that encases the entire nano-wire array. The MAPD obtained in this glass-filled photonic crystal falls slightly below the Lambertian benchmark.^{16,17} However, we show below that by removing the SiO_2 packaging, reflection losses are reduced and the resulting MAPD in fact exceeds the $4n^2$ Lambertian limit.

In Fig. 9 we compare the dependence of the maximal short circuit current on the equivalent bulk thickness of GaAs in the spectral range [400–860 nm] for air and glass packaging, respectively. It is seen that the red curve, corresponding to air packaging, rapidly approaches the limit of 100% absorption when more than 300 nm of GaAs is used. For example, 99.7% of incoming sunlight in the specified spectral range is absorbed for the equivalent bulk thickness of 500 nm. The MAPD achieved without SiO_2 packaging exceeds the Lambertian limit for any equivalent bulk thickness greater than 150 nm.

In order to clarify the nature of absorption, we plot the absorption distribution inside our conical nanowire using formula (2) and the corresponding Poynting vector distribution. For three different wavelengths (400, 600 and 850 nm) the absorption profiles are shown in Fig. 10 on a slice passing through the center of the cone (showing its symmetric triangular profile).

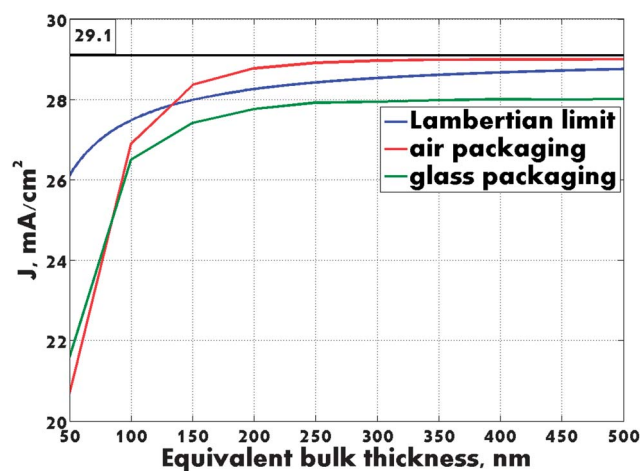


Fig. 9 Short circuit current dependence on the equivalent bulk thickness of GaAs in the spectral range [400–860 nm] for glass packaging (green curve) and air filling (red curve). The straight conical nanowire base radius is $r = 100$ nm and the lattice constant is $a = 500$ nm which is optimal for an equivalent bulk thickness of 200 nm. Further optimization may be possible at other thicknesses. The photonic crystal slab rests on a perfect conducting back-reflector of 100 nm width. The blue curve indicates the $4n^2$ Lambertian limit and the black horizontal line corresponds to the MAPD achieved for 100% absorption of sunlight.

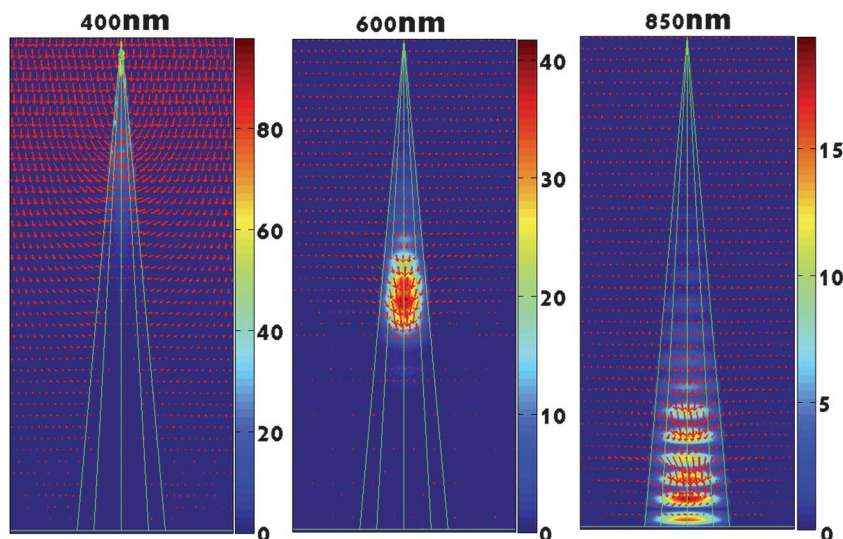


Fig. 10 Orthogonal slice for the Poynting vector and the absorption distribution in gallium arsenide for the 200 nm equivalent bulk thickness conical nanowire photonic crystal (in glass) at three different wavelengths: 400, 600 and 850 nm, respectively. The color bar on the right hand side indicates the intensity enhancement relative to a plane wave with the equivalent input power.

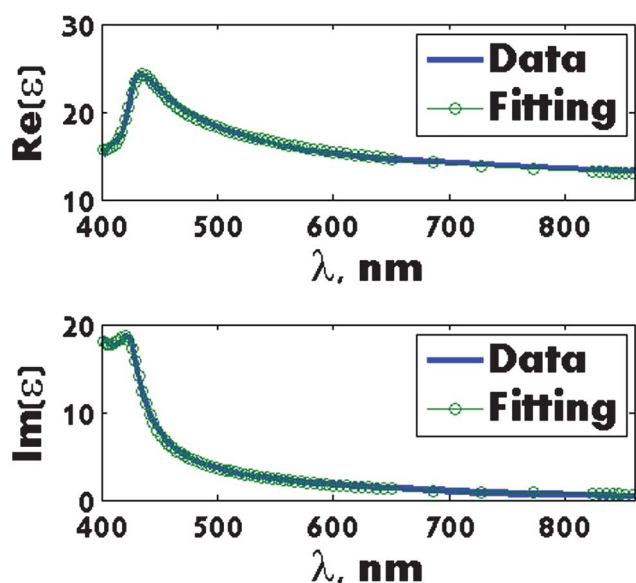


Fig. 11 Fitting of the real and imaginary parts of the frequency dependent dielectric function of bulk crystalline GaAs over the wavelength range from 400 to 860 nm. The solid blue curve represents experimental data⁵ and the open circles represent our fit to these data.

Fig. 10 reveals that the absorption in our structure occurs through strong light focusing in certain areas. The absorption distribution shows hot spots with Poynting vector convergence into these areas. The resulting high energy concentration enhances the absorption in these regions. The position of these spots depends on the wavelength. Shorter wavelengths are absorbed closer to the tip of the cone (see the left panel in Fig. 10), while wavelengths closer to the electronic band gap of gallium arsenide are absorbed closer to the bottom (see the right panel). Similar slices of the energy density distribution at other wavelengths reveal that almost all sunlight is

concentrated within the interior part of the nanowire and is spectrally separated along its length.

Finally, we consider absorption in our nanowire photonic crystal using a silver substrate and we recalculate the MAPD according to (2) and (3). Absorption within GaAs according to (2) gives the MAPD of 26.8 mA cm^{-2} , which corresponds to 93% absorption of all available sunlight in the wavelength range 400–860 nm. We conclude that for a GaAs conical nanowire photonic crystal, the overall absorption can be slightly higher (about 3%) than with nano-pore arrays.

7. Conclusion

In conclusion we have demonstrated the efficacy of gallium arsenide solar cell architectures based on slanted conical-pore and straight conical nanowire photonic crystals for near complete absorption of sunlight. From a theoretical perspective, nearly 100% absorption of sunlight in the 400–860 nm is attainable with only 300 nm of GaAs, sculpted in the form of a conical nano-wire photonic crystal. The fraction of sunlight drops to about 93% when the equivalent bulk thickness of this GaAs is reduced to 100 nm. From a practical perspective, with 200 nm of GaAs and suitable solar cell packaging, it is possible to absorb roughly 90% of sunlight in the same wavelength range. This suggests that GaAs photonic crystal solar cells can achieve about the same power conversion efficiencies as the best available thick solar cells, but with less than one-tenth the amount of GaAs.

Replacing the nano-pore array with a photonic crystal of gallium arsenide conical nanowires leads to solar absorption beyond the $4\pi^2$ Lambertian limit when the nanowires stand in air background. In a more practical solar cell architecture with suitable packaging, this absorption is slightly reduced. For an equivalent bulk thickness of GaAs of $0.2 \mu\text{m}$, we obtained a

maximal short circuit current $J = 26.9 \text{ mA cm}^{-2}$ when the nanowires are packaged in SiO_2 and placed on a silver back-reflector. This corresponds to 93% of absorption of incoming sunlight in the wavelength range [400–860 nm], which is slightly higher (about 3%) than the optimized nano-pore array. The GaAs conical nanowire photonic crystal exhibits strong solar absorption over a broad range of cone parameters. This is quite advantageous for realistic structures in which some degree of imperfection in fabrication is inevitable.

The power conversion efficiency of the corresponding GaAs photonic crystal solar cells can be estimated using coupled electromagnetic and charge carrier transport modeling. This is readily performed by EMTL,¹⁹ which provides the photo-generation source term for solution of the semiconductor drift-diffusion equation.^{6,35} In this process a further optimization of the P–N junction and contact geometries can be performed. This will be published elsewhere. It is also of considerable interest to evaluate the effects of photon recycling,^{7,36} where carriers recombine radiatively, luminesce into photonic crystal cavity modes, and then regenerate carriers. Upconversion of sunlight at wavelengths larger than 860 nm may also be realized using a layer of dye-sensitized nano-crystals^{8,37} placed near the bottom of GaAs solar cells. These two effects may help raise the power conversion efficiency of ultra-thin GaAs photonic crystal, single-junction solar cells to well beyond 30%.

Appendix

The frequency dependence of dielectric permeability $\varepsilon(\omega)$ is assigned in the FDTD method by considering a modified Lorentz model where dielectric polarization depends both on the electric field and its first time derivative.³⁸ This model provides an accurate fit of the optical response of bulk crystalline GaAs to sunlight over the wavelength range from 400 to 860 nm, while conventional Debye, Drude and Lorentz approximations fail. Fitting of the dielectric function is performed using three modified Lorentz terms with the help of an open-source MatLab program.³⁹ We find that three ($P = 3$) simple susceptibilities of the form

$$\varepsilon(\omega) = 1 - \sum_{p=1}^3 \frac{\Delta\varepsilon_p(\omega_p^2 - i\gamma'_p\omega)}{\omega_p^2 - 2i\gamma_p\omega - \omega^2}$$

are sufficient to model the entire response of bulk GaAs to sunlight over the wavelength range from 400 to 860 nm. In contrast, even a large number of Debye, Lorentz, or Drude terms are inadequate to cover the solar spectrum. We fit the GaAs permittivity with the following parameters (ω_p , γ_p , and γ'_p are in $1 \mu\text{m}^{-1}$, and the speed of light is unity):

$$\Delta\varepsilon_1 = 0.024020 \quad \omega_1 = 0.002376 \quad \gamma_1 = 0.000466 \quad \gamma'_1 = 0.769021$$

$$\Delta\varepsilon_2 = 9.624197 \quad \omega_2 = 0.002280 \quad \gamma_2 = 0.000813 \quad \gamma'_2 = 0.000003$$

$$\Delta\varepsilon_3 = 0.284488 \quad \omega_3 = 0.002349 \quad \gamma_3 = 0.000057 \quad \gamma'_3 = 0.000971$$

The result of fitting for GaAs is shown in Fig. 11.

Acknowledgements

This work is supported in part by the United States Department of Energy under contract DE-FG02-10ER46754.

References

- 1 J. Grandier, D. M. Callahan, J. N. Munday and H. A. Atwater, Gallium Arsenide Solar Cell Absorption Enhancement Using Whispering Gallery Modes of Dielectric Nanospheres, *IEEE J. Photovoltaics*, 2012, **2**(2), 123.
- 2 G. J. Bauhuis, *et al.*, Thin film GaAs solar cells with increased quantum efficiency due to light reflection, *Sol. Energy Mater. Sol. Cells*, 2004, **83**, 81–90.
- 3 C. O. McPheeters, *et al.*, Semiconductor heterostructures and optimization of light-trapping structures for efficient thin-film solar cells, *J. Opt.*, 2012, **14**, 024007.
- 4 M. A. Green, Ag requirements for silicon wafer-based solar cells, *Prog. Photovoltaics*, 2011, **19**, 911–916.
- 5 E. D. Palik, *Handbook of Optical Constants of Solids*, Academic Press, 1985.
- 6 M. A. Green, K. Emery, Y. Hishikawa and W. Warta, Solar cell efficiency tables, *Prog. Photovoltaics*, 2010, **18**, 346–352.
- 7 O. D. Miller, E. Yablonovitch and S. R. Kurtz, Intense Internal and External Fluorescence as Solar Cells Approach the Shockley-Queisser Efficiency Limit, arXiv:1106.1603v3, 2011.
- 8 E. Garnett and P. Yang, Light Trapping in Silicon Nanowire Solar Cells, *Nano Lett.*, 2010, **10**(3), 1082–1087.
- 9 Z. Yu, A. Raman and S. Fan, Fundamental limit of light trapping in grating structures, *Opt. Express*, 2010, **18**, 366–380.
- 10 A. Deinega, I. Valuev, B. Potapkin and Yu. Lozovik, Minimizing light reflection from dielectric textured surfaces, *J. Opt. Soc. Am. A*, 2011, **28**, 770–777.
- 11 P. B. Clapham and M. C. Hutley, Reduction of lens reflection by the ‘Moth Eye’ principle, *Nature*, 1973, **244**, 281–282.
- 12 W. H. Southwell, Pyramid-array surface-relief structures producing antireflection index matching on optical surfaces, *J. Opt. Soc. Am. A*, 1991, **8**, 549–553.
- 13 D. H. Raguin and G. M. Morris, Analysis of antireflection-structured surfaces with continuous one-dimensional surface profiles, *Appl. Opt.*, 1993, **32**, 2582–2598.
- 14 B. L. Sopori and R. A. Pryor, Design of antireflection coatings for textured silicon solar cells”, *Sol. Cells*, 1983, **8**, 249–261.
- 15 O. Bucci and G. Franceschetti, Scattering from wedge-tapered absorbers, *IEEE Trans. Antennas Propag.*, 1971, **19**, 96–104.
- 16 S. Eyderman, S. John and A. Deinega, Solar light trapping in slanted conical-pore photonic crystals: Beyond statistical ray trapping, *J. Appl. Phys.*, 2013, **113**, 154315.
- 17 E. Yablonovitch, Statistical ray optics, *J. Opt. Soc. Am.*, 1982, **72**(7), 899–907.
- 18 A. Taflove and S. C. Hagness, *Computational Electrodynamics: The Finite-Difference Time-Domain Method*, Artech House Publishers, 3rd edn, 2005.
- 19 *Electromagnetic Template Library (EMTL)*, Kintech Lab Ltd, <http://fdtd.kintechlab.com>.

- 20 A. Deinega and I. Valuev, Subpixel smoothing for conductive and dispersive media in the FDTD method, *Opt. Lett.*, 2007, **32**, 3429.
- 21 A. Deinega and I. Valuev, Long-time behavior of PML absorbing boundaries for layered periodic structures, *Comput. Phys. Commun.*, 2011, **182**, 149.
- 22 I. Valuev, A. Deinega and S. Belousov, Iterative technique for analysis of periodic structures at oblique incidence in the finite-difference time-domain method, *Opt. Lett.*, 2008, **33**, 1491.
- 23 <http://rredc.nrel.gov/solar/spectra/am1.5/>.
- 24 T. Y. M. Chan, O. Toader and S. John, Photonic band-gap formation by optical-phase-mask lithography, *Phys. Rev. E: Stat., Nonlinear, Soft Matter Phys.*, 2006, **73**, 046610.
- 25 N. Tetreault, G. von Freymann, M. Deubel, M. Hermatschweiler, F. Perez-Willard, S. John, M. Wegener and G. A. Ozin, *Adv. Mater.*, 2006, **18**(4), 457.
- 26 A. Vlad, A. Frölich, T. Zebrowski, C. A. Dutu, K. Busch, S. Melinte, M. Wegener and I. Huynen, Direct Transcription of Two-Dimensional Colloidal Crystal Arrays into Three-Dimensional Photonic Crystals, *Adv. Funct. Mater.*, 2013, **23**, 1164–1171.
- 27 E. Nelson, *et al.* Epitaxial growth of three-dimensionally architected optoelectronic devices, *Nat. Mater.*, 2011, **10**, 676–681.
- 28 X.-Y. Bao, *et al.* Heteroepitaxial Growth of Vertical GaAs Nanowires on Si (111) Substrates by Metal-Organic Chemical Vapor Deposition, *Nano Lett.*, 2008, **8**(11), 3755–3760.
- 29 O. Demichel, *et al.* Impact of surfaces on the optical properties of GaAs nanowires, *Appl. Phys. Lett.*, 2010, **97**, 201907.
- 30 M. Green, *Third generation photovoltaics*, Springer, Berlin, 2006.
- 31 A. Deinega, S. Eyderman and S. John, Coupled optical and electrical modeling of solar cell based on conical pore silicon photonic crystals, *J. Appl. Phys.*, 2013, **113**, 224501.
- 32 G. Demesy and S. John, Solar energy trapping with modulated silicon nanowire photonic crystals, *J. Appl. Phys.*, 2012, **112**, 074326.
- 33 A. Deinega and S. John, Solar Power Conversion Efficiency in Modulated Silicon Nanowire Photonic Crystals, *J. Appl. Phys.*, 2012, **112**, 074327.
- 34 J. Wallentin, *et al.*, InP Nanowire Array Solar Cells Achieving 13.8% Efficiency by Exceeding the Ray Optics Limit, *Science*, 2013, **339**, 1057–1060.
- 35 <https://sites.physics.utoronto.ca/sajeevjohn/software/microvolt>.
- 36 V. Badescu and P. T. Landsberg, Influence of photon recycling on solar cell efficiencies, *Semicond. Sci. Technol.*, 1997, **12**, 1491.
- 37 C. Yuan, *et al.*, Use of colloidal upconversion nanocrystals for energy relay solar cell light harvesting in the near-infrared region, *J. Mater. Chem.*, 2012, **22**, 16709–16713.
- 38 A. Deinega and S. John, Effective optical response of silicon to sunlight in the finite-difference time-domain method, *Opt. Lett.*, 2012, **37**, 112.
- 39 <http://fdtd.kintechlab.com/en/fitting>.